Structure of Al(111)-($\sqrt{3}\times\sqrt{3}$)R 30°-Na: A LEED study

J. Burchhardt, M. M. Nielsen, and D. L. Adams
Institute of Physics and Astronomy, Aarhus University, DK-8000 Aarhus C, Denmark

E. Lundgren and J. N. Andersen
Department of Synchrotron Radiation Research, Institute of Physics, Lund University, S-223 62 Lund, Sweden
(Received 23 February 1994)

The atomic geometry of the Al(111)-($\sqrt{3}\times\sqrt{3}$)R 30°-structure formed by adsorption of Na on Al(111) at room temperature has been determined by analysis of extensive low-energy electron-diffraction (LEED) measurements. It is shown conclusively that Na atoms occupy a sixfold-coordinate site formed by displacing every third Al atom in the first layer of the substrate. This confirms the results of a recent study by surface extended x-ray-absorption fine structure.

I. INTRODUCTION

A recent surface extended x-ray-absorption fine-structure (SEXAFS) study[1] of the adsorption of Na on Al(111) at room temperature revealed that the adsorption is accompanied by a reconstruction of the substrate, in which Na atoms are located in quasisubstitutional sites of sixfold coordination formed by displacing one-third of the Al atoms in the first layer. This completely unexpected result has added another dimension to the discussion of the nature of alkali-metal adsorption. It has stimulated a number of recent experimental and theoretical studies[2–10] in which the possibility of a strong perturbation of the substrate structure induced by alkali-metal adsorption has been taken into account. Thus the adsorption of K and Rb on Al(111) and the adsorption of Na on Al(100) have been shown by low-energy electron-diffraction[2,3] (LEED) and SEXAFS studies,[4] respectively, to lead to a reconstruction of the substrate. The results for these systems are supported by high-resolution core-level spectroscopy studies which, in addition, lead to the conclusion that the adsorption of Cs on Al(111) at room temperature also produces a reconstruction of the substrate.[5,6] For Na adsorption on Al(111), the SEXAFS results are supported by the results of *ab initio* calculations,[1,7] which show that the binding energy for Na atoms in the substitutional site is significantly larger than for nonreconstructive adsorption in threefold, bridge, or on-top sites. The SEXAFS results are also supported by the results of normal-incidence x-ray standing-wave (NIXSW) measurements.[10] To date, reports of strong reconstruction of close-packed metal surfaces induced by adsorption of alkali metals have been limited to Al surfaces. However, the occupation of an unusual on-top site on a rumpled first substrate layer has been reported in recent LEED studies of the adsorption of K on Ni(111) (Ref. 8) and Cs on Ru(0001).[9] Occupation of an on-top site on a rumpled substrate is also found for adsorption of K and Rb on Al(111) at low temperature.[2,3]

In view of the importance of the SEXAFS results for the Al(111)-($\sqrt{3}\times\sqrt{3}$)R 30°-Na structure, further corroboration using a different technique was clearly desirable. Thus in the present work we have carried out a detailed LEED study of this system. As described in detail below, our results confirm that Na atoms occupy quasisubstitutional sites. The determined Al-Na bond length of 3.21 Å is, however, somewhat shorter than the SEXAFS result of 3.31 Å.

In the following, the experimental procedures used in this study are described in Sec. II. The procedures used in analyzing the data, including the calculation of LEED intensities, are described in Sec. III. The results of the data analysis are presented and discussed in Sec. IV.

II. EXPERIMENTAL PROCEDURES

The measurements were carried out in a Vacuum Generators mu-metal ultrahigh vacuum chamber with base pressure of 3×10^{-11} torr. The chamber was equipped with an Omicron reverse-view LEED optics, which was used both for LEED intensity measurements and for Auger electron spectroscopy (AES) measurements of surface chemical composition. The A1(111) crystal was mounted on a manipulator with facilities for rotation of the crystal about two orthogonal axes through the nominal crystal position, and with a tilt motion of the manipulator shaft about an axis perpendicular to the shaft at the top of the manipulator. The crystal could be cooled to 100 K using liquid nitrogen and heated by electron bombardment The crystal temperature was measured using a W-5% Re/W-26% Re thermocouple spot-welded to the rear of the crystal. The crystal was cleaned by cycles of Ar^+ bombardment and annealing to 750 K.

Sodium was deposited onto the crystal by evaporation from an SAES source. The deposition was carried out in a few minutes, and the residual-gas pressure during evaporation was typically 2×10^{-10} torr. AES measurements taken after deposition and after completion of a set of LEED measurements indicated that surface contamination (almost entirely C) was less than 0.03 monolayer. Sharp ($\sqrt{3}\times\sqrt{3}$)R 30° LEED patterns with good contrast were obtained after deposition of $\frac{1}{3}$ monolayer Na at 300 K.

The LEED intensity measurements were made using a

video-LEED system, described previously,[11,12] consisting of a computer-controlled video camera and a rear-view LEED optics. A digital image of the LEED pattern with a geometric resolution of 512×512 pixels and an intensity resolution of eight bits is obtained at each energy. The intensity of a given diffracted beam is obtained from the digital image by summing the pixel intensities in a window centered on the diffraction spot. The spot intensity is corrected for background, as measured by summing pixel intensities in windows above and below the diffraction spot, and is normalized for the electron-beam current and for the Lambert's law variation of the spot intensity with its position on the fluorescent screen. The spot intensity is also corrected for the spatial variation of the camera sensitivity, as calibrated using a 99.5% homogeneous light source. The intensities of an arbitrary number of beams are measured simultaneously (to within the 40-ms digitalization time). Determination of the spot intensities is carried out in real time and requires about 40 ms per beam at a given energy. The dynamic range of the measurements is greatly increased by changing the optical gain of the system synchronously with the incident electron energy. This is achieved by programming the gain of the video amplifier of the camera at each energy, in a feedback loop, to achieve near-saturation intensity for a chosen diffraction spot. A further improvement in the signal-to-noise ratio is obtained by dividing the beams into two sets according to their average intensities, making separate measurements for each set, and programming the camera gain to achieve near-saturation intensity for the brightest beam of the set of interest at each energy. The intensity-energy spectra shown later have been normalized for the video gain, and are therefore on the same accurately known (but arbitrary) intensity scale.

Intensity-energy spectra were measured at 100 K, in the energy range 40–450 eV, at normal incidence $\theta=0°$, for the clean Al(111) surface, and in the energy range 40–400 eV at $\theta=0°$ and $-15°$ for the ($\sqrt{3}\times\sqrt{3}$)R30°-Na structure. The azimuthal angle of the crystal was set at 0° for the measurements at $\theta=-15°$, such that the plane of incidence coincided with a mirror plane of the surface structure. The incidence angles were set to within ±0.1° by minimizing the R factor (see below) for the comparison of intensity-energy spectra for (nominally) symmetry-equivalent beams. As in previous studies[2,3,12] using the present system, it was found that discrepancies between spectra for symmetry-equivalent beams were larger than the random errors between repetitive measurements for the same beam. The spectra shown below are the result of averaging over five sets of measurements of the individual hk beams, followed by smoothing, followed by averaging the intensities of symmetry-equivalent beams. The experimental data base is summarized in Table I.

TABLE I. Experimental data base for clean Al(111) and Al(111)-($\sqrt{3}\times\sqrt{3}$)R30°-Na. $R_{\text{exp-exp}}$ is the R factor for the comparison of symmetry-equivalent beams.

	(1×1)	($\sqrt{3}\times\sqrt{3}$)R30°-Na	
Angle of incidence	0°	0°	−15°
Energy range	50–450 eV	40–400 eV	40–400 eV
Energy grid	1eV	1eV	1eV
Total number of beams	16	48	35
Symmetry inequivalent Integral order beams	5	5	9
Symmetry inequivalent Fractional order beams	0	7	16
$R_{\text{exp-exp}}$	0.007	0.029	0.011

III. LEED CALCULATIONS AND R-FACTOR ANALYSIS

LEED intensities were calculated using the dynamical theory of LEED, with computer programs derived from the layer-doubling and combined-space programs of Pendry[13] and Van Hove and Tong.[14] Atomic scattering matrices for Al and Na were calculated using phase shifts calculated from the muffin-tin band-structure potentials of Moruzzi, Janak, and Williams,[15] and were renormalized for the effects of thermal vibrations using root-mean-square (rms) isotropic vibrational amplitudes u_{Na} for the adsorbed Na atoms, $u_{\text{Al},1}$ for the first Al layer, and $u_{\text{Al,bulk}}$ for the Al substrate. Up to 196 partial waves (14 phase shifts) and 253 plane waves (reduced respectively to 47 and 129 symmetry-adapted plane waves at $\theta=0°$ and $-15°$) were used respectively in the L- and k-space treatments of multiple scattering within and between layers parallel to the surface. The complex electron self-energy $\Sigma=V_0+iV_{\text{im}}$ was taken to be independent of energy. The surface potential barrier was taken to be a refracting but nonreflecting step of height V_0, positioned at a distance equal to one-half the bulk interlayer spacing above the first layer of atoms. We estimate that the calculations are a numerically accurate reflection of the model assumptions to about 0.1%. All calculations used in the structure determination were carried out with full accuracy.

Refinement of the surface structures of clean Al(111) and Al(111)-($\sqrt{3}\times\sqrt{3}$)R30°-Na was carried out using an automatic implementation of a simple, iterative procedure described previously,[16] which makes extensive reuse of scattering matrices, which are stored for all energies, for the individual layers, selvedge, and bulk of the crystal. Thus in each complete iteration, carried out in a single computer run, the optimum values of the first four interlayer spacings d_i and V_0 were determined by minimizing the R factor as a function of each layer spacing in turn for fixed values of the remaining nonstructural parameters V_{im}, u_{Na}, $u_{\text{Al},1}$, and $u_{\text{Al,bulk}}$. In each elementary step the optimum value of a particular layer spacing was determined simultaneously with V_0. The procedure was iterated to convergence, which typically required 3–5 passes with the convergence condition that $\sum_{i=0,3}|\Delta d_i|\leq 0.001$ Å, where Δd_i is the change in the optimum value of d_i from one iteration to the next. The remaining nonstructural parameters were varied in an outer loop of the refinement, which was also iterated to convergence.

The calculations, which were carried out on a Digital DEC Alpha workstation, required about 5 min for the automatic determination of the optimum values of the

first four interlayer spacings and V_0, after first calculating k-space, layer-scattering matrices and the bulk reflection matrix at all energies on an energy grid of 0.3 Ry. The calculation of scattering matrices for Na and Al layers at all energies required about 2 min per different layer, except for the scattering matrices for a reconstructed Al layer, which required about 30 min.

The surface structures were determined by minimizing the R factor for the comparison of experimental $I_{hk}^{\rm exp}(E)$ and calculated $I_{hk}^{\rm cal}(E)$ intensity-energy spectra as a function of the structural and nonstructural variables of the calculations defined above. The R factor used here is a normalized χ^2 function defined[12,16] as

$$R=\sum_{hk,i}\left[\frac{I_{hk,i}^{\rm exp}-cI_{hk,i}^{\rm cal}}{\sigma_{hk}}\right]^2\Big/\sum_{hk,i}\left[\frac{I_{hk,i}^{\rm exp}}{\sigma_{hk}}\right]^2, \quad (1)$$

where c is a single, global scaling constant between the experimental and calculated intensities determined by the requirement that $\partial R/\partial c=0$, and σ_{hk} are the beam-average rms uncertainties obtained by comparison[12] of experimental intensity spectra for symmetry-equivalent beams. The R factor for the individual hk beams is defined as

$$r_{hk}=\sum_i (I_{hk,i}^{\rm exp}-cI_{hk,i}^{\rm cal})^2\Big/\sum_i (I_{hk,i}^{\rm exp})^2 . \quad (2)$$

From these definitions it follows that strong and weak beams contribute to the R factor on an equal footing. However, beams with relatively large errors (σ_{hk}) are downweighted. Estimation of the uncertainties in the best-fit values is obtained from[12]

$$\sigma_j^2=2kR_{\rm min}/\partial^2 R/\partial x_j^2 , \quad (3)$$

where the constant k is taken to be 0.1. As illustrated below in Fig. 3, this recipe amounts to equating σ_j with the change Δx_j in the optimum value $x_j^{\rm opt}$ that corresponds to a 10% increase in R from $R_{\rm min}$.

IV. RESULTS AND DISCUSSION

A. Clean Al(111)

The results of the refinement of the structure of clean Al(111) are given in Table II. As can be seen from the table, the surface structure almost corresponds to the truncation of a perfect bulk crystal. A small expansion (+1.4%) is found for the first interlayer spacing, in agreement with previous studies.[17–19] However, the rms vibrational amplitudes of Al atoms in the first layer are enhanced by about 60% over the corresponding amplitudes for Al atoms in the second and deeper layers. This finding is similar to results obtained recently by some of the present authors[12] for clean Ni(100), and is in partial agreement with the results of a study of clean Al(111) at

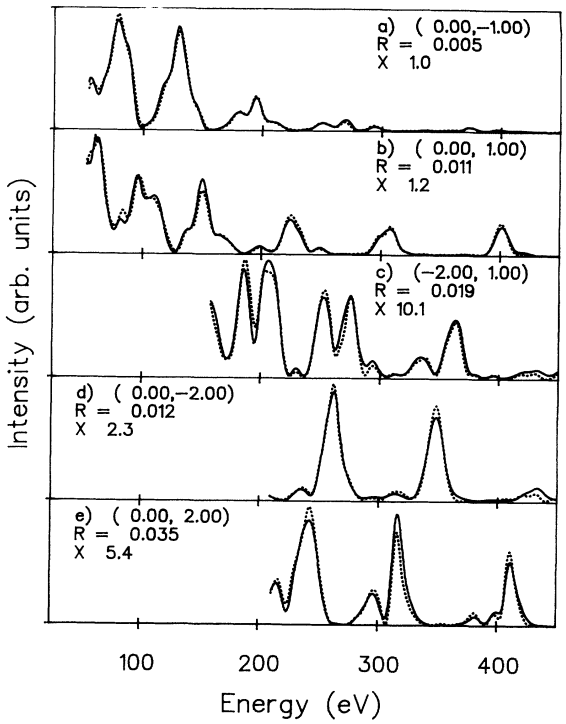

FIG. 1. Comparison of experimental (solid lines) and calculated (dotted lines) intensity-energy spectra for clean Al(111) at $\theta=0°$ for five diffracted beams, (a)–(e). The calculated spectra were obtained using the best-fit parameter values given in Table II. Each panel shows the hk indices, the R-factor values for the comparison, and scale factors which must be applied to place the spectra for the different beams on the same intensity scale.

TABLE II. Best-fit parameter values for clean Al(111) and for Na adsorbed in the quasisubstitutional site in the Al(111)-$(\sqrt{3}\times\sqrt{3})R30°$-Na structure. d_j is the spacing between layers j and $j+1$ in the surface-normal direction. d_0 is the Na-Al spacing. The values for d_3 were in all cases equal to the value for bulk Al within the precision of the determinations. $r_{\rm Na}$ is the effective hard-sphere radius for Na, assuming $r_{\rm Al}=1.426$ Å. $u_{\rm Na}$, $u_{\rm Al,1}$, and $u_{\rm Al,bulk}$ are the rms vibrational amplitudes for Na atoms, Al atoms in the first layer, and Al atoms in the bulk, respectively.

	(1×1)	$(\sqrt{3}\times\sqrt{3})R30°$-Na	
Angle of incidence	0°	0°	−15°
d_0		1.47±0.02 Å	1.48±0.02 Å
d_1	2.36±0.01 Å	2.27±0.02 Å	2.24±0.03 Å
d_2	2.33±0.01 Å	2.32±0.02 Å	2.34±0.03 Å
$u_{\rm Na}$		0.23±0.02	0.24±0.03
$u_{\rm Al,1}$	0.13±0.02 Å	0.13±0.02 Å	0.11±0.03 Å
$u_{\rm Al,bulk}$	0.08±0.01 Å	0.10±0.01 Å	0.10±0.02 Å
$V_{\rm im}$	4.0±0.4 eV	3.6±0.6 eV	3.4±0.6 eV
R	0.009	0.029	0.049

160 K by Noonan and Davis.[19] The Debye temperatures reported by the latter authors correspond to rms vibrational amplitudes at 160 K of $u_{Al,1}=0.11$ Å and $u_{Al,bulk}=0.09$ Å, as compared to the values of 0.13 ± 0.02 and 0.08 ± 0.01 Å found here at 100 K. From an analysis in which the vibrational amplitudes of the first two Al layers were allowed to differ from the bulk value, Noonan and Davis reported values of $u_{Al,1}=0.13$ Å, $u_{Al,2}=0.12$ Å, and $u_{Al,bulk}=0.08$ Å. The values found here in a corresponding analysis are $u_{Al,1}=0.13\pm0.02$ Å, $u_{Al,2}=0.07\pm0.02$ Å, and $u_{Al,bulk}=0.09\pm0.01$ Å.

A comparison of the experimental intensity-energy spectra with spectra calculated for the optimum parameter values given in Table II is shown in Fig. 1. The agreement between experiment and calculations is at the level of the reproducibility of the measurements. The R factor for the comparison is 0.011, as compared to the value of 0.007 obtained from the comparison of experimental spectra for symmetry-equivalent beams.

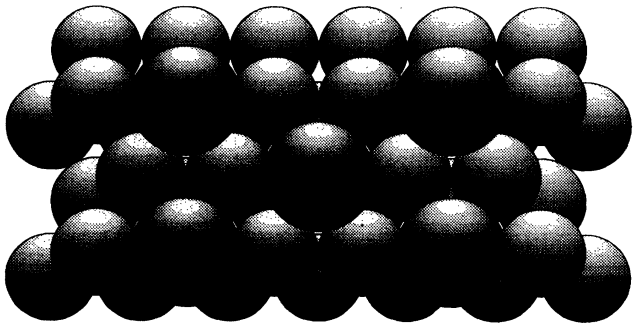

a) Na in 6-fold quasisubstitutional site
Top View

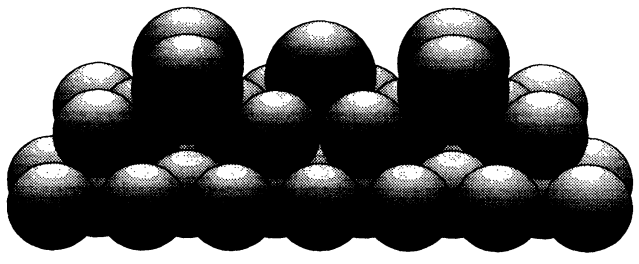

b) Side View (tilted 10°)

FIG. 2. Hard-sphere model of the geometry of the Al(111)-($\sqrt{3}\times\sqrt{3}$)R30°-Na structure. The larger circles represent Na atoms adsorbed in the quasisubstitutional site: (a) top view; (b) side view, shown as a central projection on the [11$\bar{2}$] plane tilted by 10° with respect to the plane of the paper.

B. Al(111)-($\sqrt{3}\times\sqrt{3}$)R30°-Na

In the initial stage of the structure determination, a preliminary survey was carried out of structural models involving Na atoms adsorbed in onefold on-top sites, threefold hollow fcc and hcp sites, and sixfold quasisubstitutional sites (see Fig. 2), compatible with the symmetry of the measured LEED intensities. Although no optimization of the nonstructural parameters was carried out in this survey, the results indicated unequivocally that only the sixfold substitutional site warranted further refinement.

A full optimization of the fit between experimental intensities and intensities calculated for the substitutional site was carried out using the procedure described in Sec. III. The dependence of the fit on the interlayer spacings d_0 and d_1 and the rms vibrational amplitudes u_{Na}, $u_{Al,1}$, and $u_{Al,bulk}$ is shown in Fig. 3. Although the fit is clearly much more sensitive to the structural parameters than to the nonstructural parameters, it can be seen from the figure that the R factor is a well-behaved, parabolic function of u_{Na}, $u_{Al,1}$, and $u_{Al,bulk}$, which leads to good precision in determination of their optimum values. The intersections of the horizontal line at $R=1.1\,R_{min}$, where R_{min} is the optimum value of R, with the curves for d_0, d_1, u_{Na}, $u_{Al,1}$, and $u_{Al,bulk}$, yield the estimated uncertainties for these parameters.

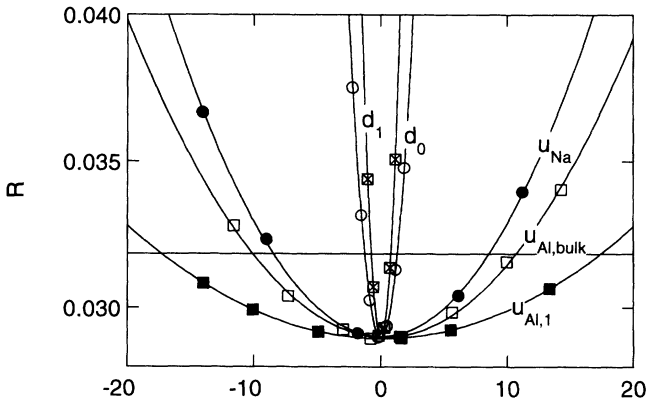

FIG. 3. Plots of the R factor for the comparison of experimental and calculated intensity-energy spectra for Al(111)-($\sqrt{3}\times\sqrt{3}$)R30°-Na at $\theta=0°$ as a function of the Na-Al interlayer spacing d_0, the first Al-Al interlayer spacing d_1, and the rms vibrational amplitudes u_{Na}, $u_{Al,1}$, and $u_{Al,bulk}$ for atoms in the adsorbed Na layer, the first reconstructed Al layer, and the Al substrate, respectively. The variables are shown as percentage changes Δx_j from their optimum values x_j^{opt}. The horizontal line in the figure is at $R=1.1\,R_{min}$, where R_{min} is the minimum value of R. The estimated uncertainties in the best-fit parameter values given in Table II correspond to the values of Δx_j at the intersection of the line at $R=1.1\,R_{min}$, with the curves in the figure. Note the much larger sensitivity of the R factor to the structural variables. Note also the well-behaved, parabolic variation of R with the variables. (The curves shown are obtained by least-squares fitting of the data points to a second-order polynomial.)

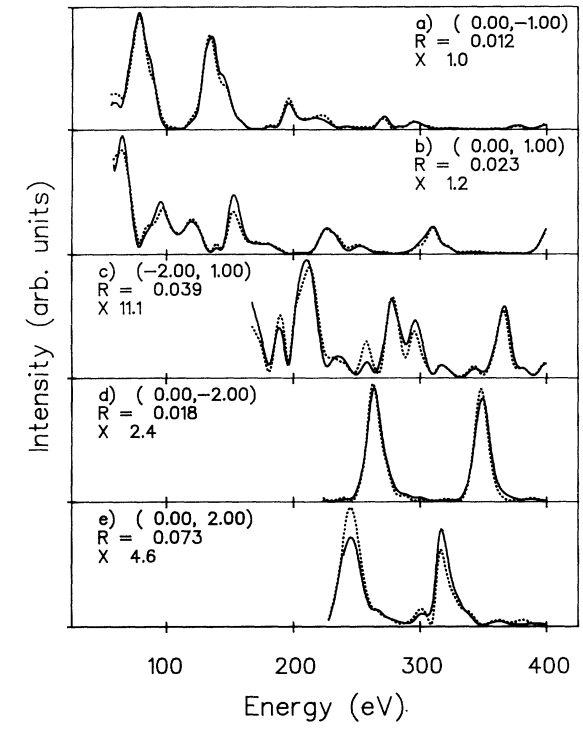

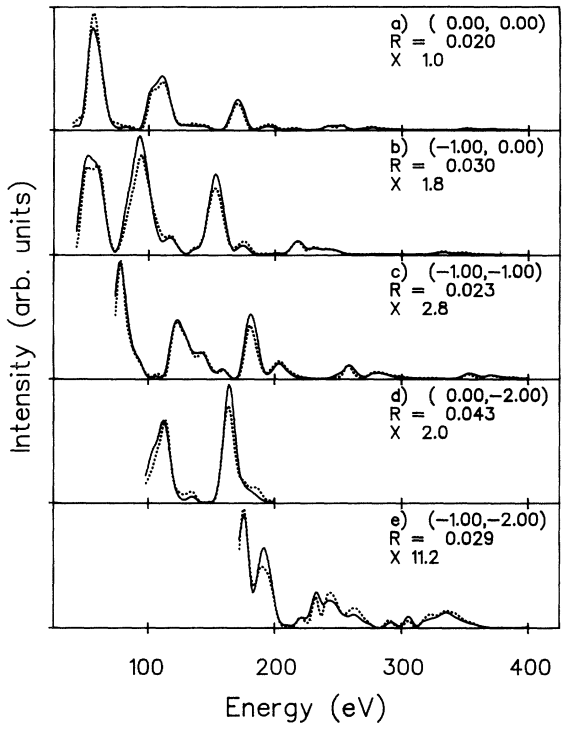

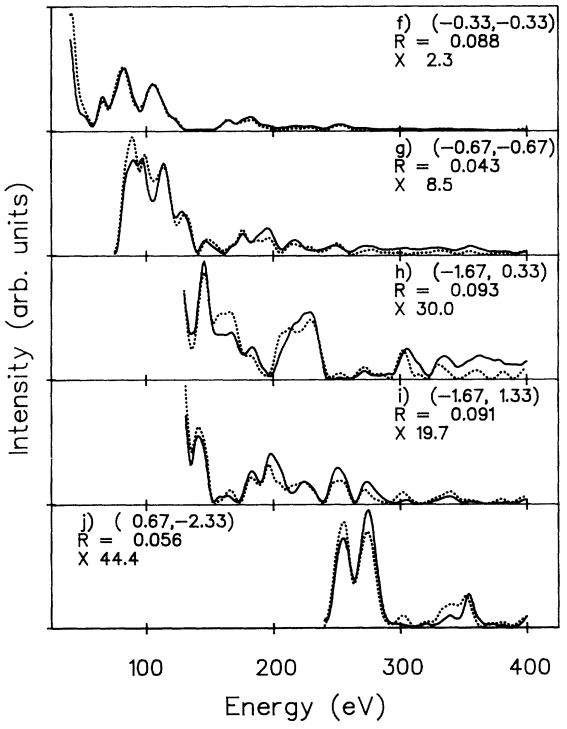

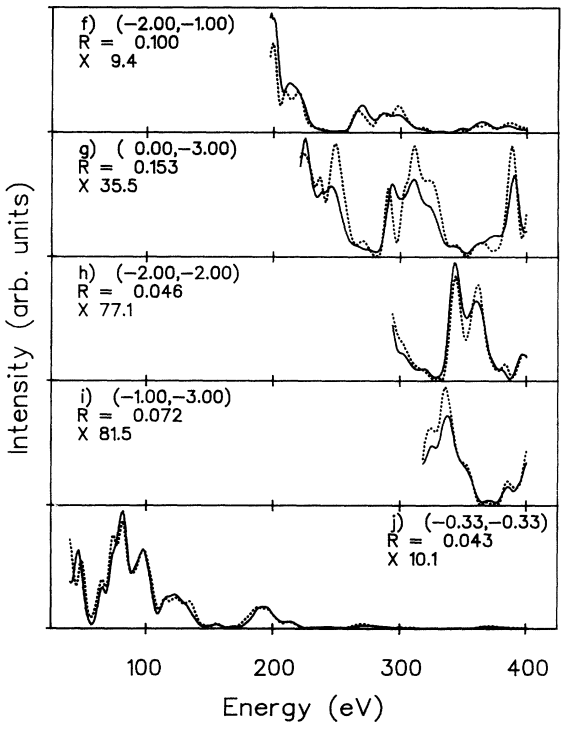

FIG. 4. Comparison of experimental (solid lines) and calculated (dotted lines) intensity-energy spectra for Al(111)-$(\sqrt{3}\times\sqrt{3})R30°$-Na at $\theta=0°$ for five integral-order beams, (a)–(e), and five fractional order beams, (f)–(j). The beam hk indices, R factors, and scale factors are shown in each panel. The calculated spectra were obtained using the best-fit parameter values given in Table II.

FIG. 5. Comparison of experimental (solid lines) and calculated (dotted lines) intensity-energy spectra for Al(111)-$(\sqrt{3}\times\sqrt{3})R30°$-Na at $\theta=-15°$ for nine integral-order beams, (a)–(i), and 16 fractional order beams, (j)–(y). The beam hk indices, R factors, and scale factors are shown in each panel. The calculated spectra were obtained using the best-fit parameter values given in Table II.

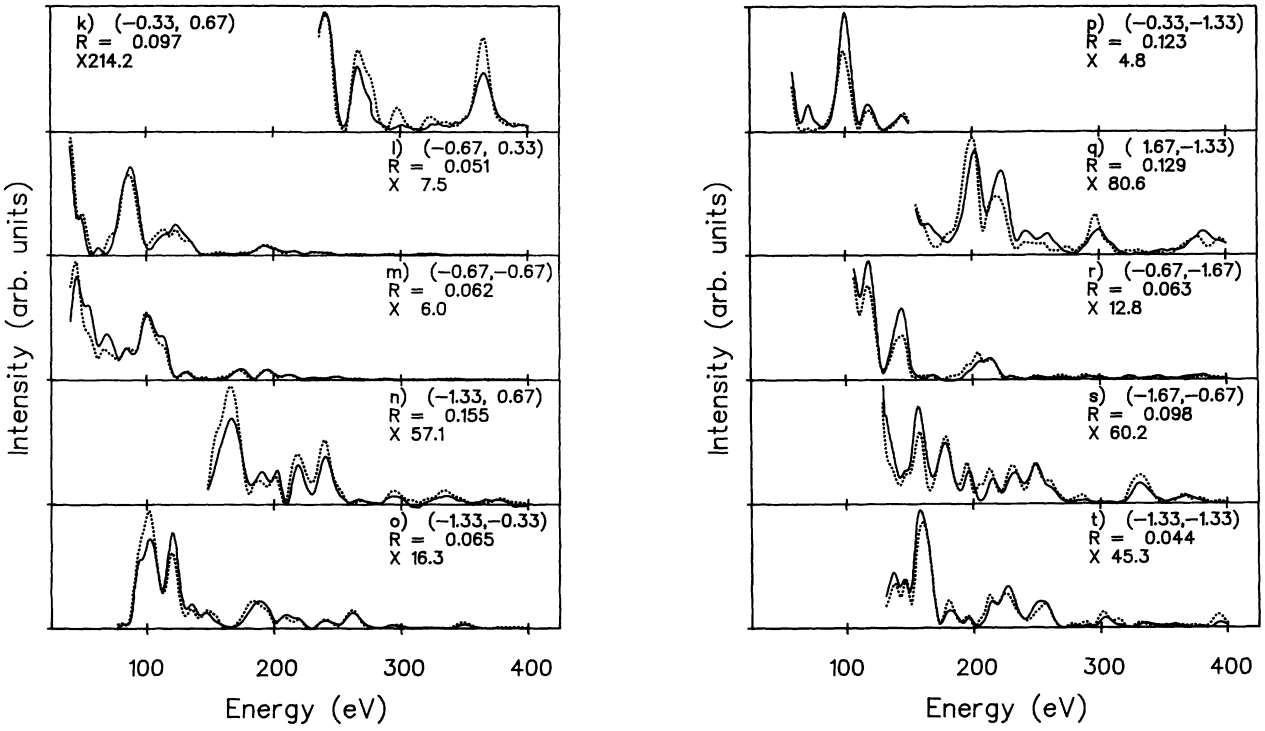

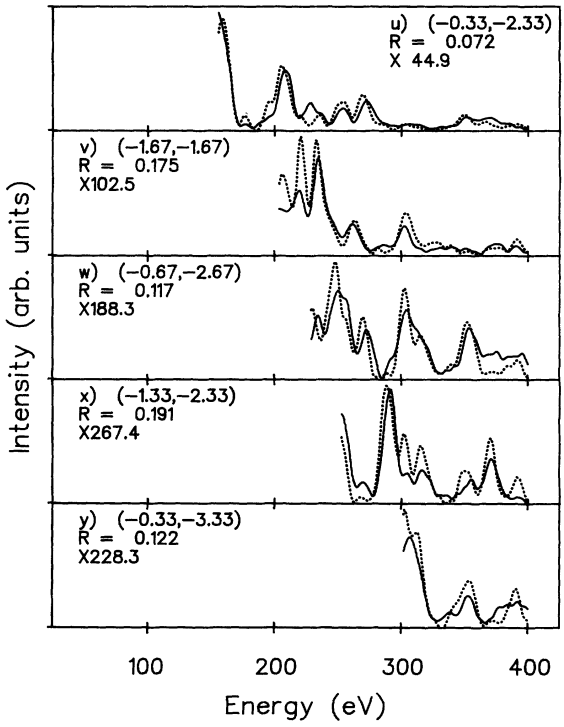

FIG. 5. (Continued).

The results of the refinement for the substitutional site are listed in Table II. Separate, full optimizations were carried out for the data sets at $\theta=0°$ and $-15°$, respectively. As can be seen from the table, the Na-Al interlayer spacing is 1.47 ± 0.02 Å, corresponding to a Na-Al bond length of 3.21 Å, and an effective hard-sphere radius of 1.78 Å for the adsorbed Na atoms. The spacing between the reconstructed, first Al layer and the next Al layer is about 3% less than the bulk Al-Al interlayer spacing. The vibrational amplitudes of Al atoms in the first layer and subsequent layers, respectively, are essentially unchanged from their values in the clean Al(111) surface. The final structural model is sketched in Fig. 3.

Plots of experimental intensity spectra and spectra calculated for the optimum parameter values given in Table II are shown in Figs. 4 and 5 for $\theta=0°$ and $-15°$ respectively. The agreement between experiment and calculations is at or close to the level of the reproducibility of the measurements. The R factors for the comparisons are 0.029 and 0.049, as compared to the values of 0.029 and 0.011, respectively for $\theta=0°$ and $-15°$, obtained from the comparisons of experimental spectra for symmetry-equivalent beams. We note that the plots have been constructed using a single, beam-independent scaling factor between experiment and calculations. Thus the very good agreement between experiment and calculations also includes agreement between the relative intensities of the different hk beams. As can be seen from the scale factors in Figs. 4 and 5, the maximum intensities of the different beams span a range of 44 and 267 at $\theta=0°$ and $-15°$, respectively.

In summary, the present LEED determination of the geometry of the Al(111)-$(\sqrt{3}\times\sqrt{3})R30°$-Na structure confirms the conclusion of a previous SEXAFS study[1] that Na atoms are adsorbed in sixfold, quasisubstitutional sites formed by displacing one-third monolayer Al atoms from the first layer of the substrate. It is further found here that adsorption of Na induces a contraction of 3% in the spacing between the first two Al layers. The Na-Al bond length[20] of 3.21 ± 0.01 Å determined here lies between the values of 3.31 ± 0.03 Å found in the SEXAFS study, the value of 3.09 ± 0.06 Å found in the NIXSW study,[10] and the value of 3.13 Å found in the calculations of Neugebauer and Scheffler.[1,7]

ACKNOWLEDGMENTS

The authors thank Jochen Haase and Matthias Scheffler for useful discussions. Support of this work by the Danish Natural Science Research Council and Center for Surface Reactions, and by the Swedish Natural Science Research Council, and NORFA is gratefully acknowledged.

[1]A. Schmalz, S. Aminpirooz, L. Becker, J. Haase, J. Neugebauer, M. Scheffler, D. R. Batchelor, D. L. Adams, and E. Bøgh, Phys. Rev. Lett. **67**, 2163 (1991).

[2]C. Stampfl, M. Scheffler, H. Over, J. Burchhardt, M. M. Nielsen, D. L. Adams, and W. Moritz, Phys. Rev. Lett. **69**, 1532 (1992); Phys. Rev. B **49**, 4959 (1994).

[3]M. M. Nielsen, J. Burchhardt, D. L. Adams, E. Lundgren, and J. N. Andersen, Phys. Rev. Lett. **72**, 3370 (1994).

[4]S. Aminpirooz, A. Schmalz, L. Becker, N. Pangher, J. Haase, M. M. Nielsen, D. R. Batchelor, E. Bøgh, and D. L. Adams, Phys. Rev. B **46**, 15 594 (1992).

[5]J. N. Andersen, M. Qvarford, R. Nyholm, J. F. van Acker, and E. Lundgren, Phys. Rev. Lett. **68**, 94 (1992).

[6]J. N. Andersen, E. Lundgren, R. Nyholm, and M. Qvarford, Surf. Sci. **289**, 307 (1993).

[7]J. Neugebauer and M. Scheffler, Phys. Rev. B **46**, 16 067 (1992).

[8]D. Fisher, S. Chandavarker, I. R. Collins, R. D. Diehl, P. Kaukasoina, and M. Lindroos, Phys. Rev. Lett. **68**, 2786 (1992).

[9]H. Over, H. Bludau, M. Skottke-Klein, G. Ertl, W. Moritz, and C. T. Campbell, Phys. Rev. B **45**, 8638 (1992).

[10]M. Kerkar, D. Fisher, D. P. Woodruff, R. G. Jones, R. D. Diehl, and B. Cowie, Phys. Rev. Lett. **68**, 3204 (1992); Surf. Sci. **278**, 246 (1992).

[11]D. L. Adams, S. P. Andersen, and J. Burchhardt, in *The Structure of Surfaces III,* edited by S. Y. Tong, M. A. Van Hove, X. Xide, and K. Takayanagi (Springer, Berlin, 1991), p. 156.

[12]M. M. Nielsen, J. Burchhardt, and D. L. Adams, Phys. Rev. B (to be published).

[13]J. B. Pendry, *Low Energy Electron Diffraction* (Academic, London, 1974).

[14]M. A. Van Hove and S. Y. Tong, *Surface Crystallography by LEED* (Springer-Verlag, Berlin, 1979).

[15]V. L. Moruzzi, J. F. Janak, and A. R. Williams, *Calculated Electronic Properties of Metals* (Pergamon, New York, 1978).

[16]D. L. Adams, V. Jensen, X. F. Sun, and J. H. Vollesen, Phys. Rev. B **38**, 7913 (1988).

[17]F. Jona, D. Sondericker, and P. Marcus, J. Phys. C **13**, L155 (1980).

[18]H. B. Nielsen and D. L. Adams, J. Phys. C **15**, 615 (1982).

[19]J. R. Noonan and H. L. Davis, J. Vac. Sci. Technol. A **8**, 2671 (1990).

[20]Except for the SEXAFS result, the quoted values of the Na-Al bond length and uncertainties are derived from the corresponding values for the Na-Al interlayer spacings. In the case of the NIXSW result, we have corrected the reported value of the Na-Al interlayer spacing of 1.20 Å for the cumulative relaxation of the Al layers in the selvedge, determined here to be 0.07 Å.

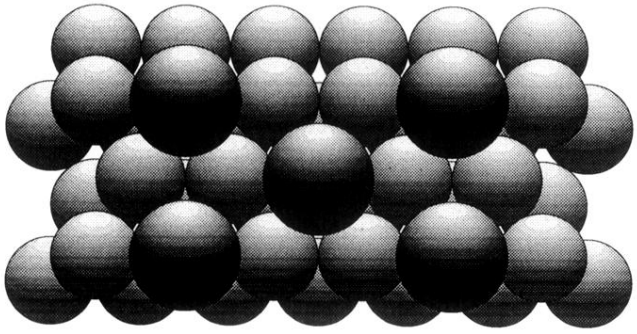

a) Na in 6-fold quasisubstitutional site
Top View

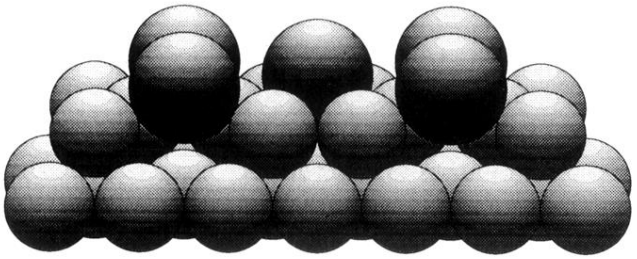

b) Side View (tilted 10°)

FIG. 2. Hard-sphere model of the geometry of the Al(111)-$(\sqrt{3}\times\sqrt{3})R30°$-Na structure. The larger circles represent Na atoms adsorbed in the quasisubstitutional site: (a) top view; (b) side view, shown as a central projection on the $[11\bar{2}]$ plane tilted by 10° with respect to the plane of the paper.